OPEN

Oncogene (2017) **36**, 3651–3660

www.nature.com/onc

ORIGINAL ARTICLE

Macrophages confer survival signals via CCR1-dependent translational MCL-1 induction in chronic lymphocytic leukemia

MHA van Attekum[1,2], S Terpstra[1,2], E Slinger[1,2], M von Lindern[3], PD Moerland[4], A Jongejan[4], AP Kater[1,5,6] and E Eldering[2,5,6]

Protective interactions with bystander cells in micro-environmental niches, such as lymph nodes (LNs), contribute to survival and therapy resistance of chronic lymphocytic leukemia (CLL) cells. This is caused by a shift in expression of B-cell lymphoma 2 (BCL-2) family members. Pro-survival proteins B-cell lymphoma-extra large (BCL-X_L), BCL-2-related protein A1 (BFL-1) and myeloid leukemia cell differentiation protein 1 (MCL-1) are upregulated by LN-residing T cells through CD40L interaction, presumably via nuclear factor (NF)-κB signaling. Macrophages (Mϕs) also reside in the LN, and are assumed to provide important supportive functions for CLL cells. However, if and how Mϕs are able to induce survival is incompletely known. We first established that Mϕs induced survival because of an exclusive upregulation of MCL-1. Next, we investigated the mechanism underlying MCL-1 induction by Mϕs in comparison with CD40L. Genome-wide expression profiling of *in vitro* Mϕ- and CD40L-stimulated CLL cells indicated activation of the phosphoinositide 3-kinase (PI3K)-V-Akt murine thymoma viral oncogene homolog (AKT)-mammalian target of rapamycin (mTOR) pathway, which was confirmed in *ex vivo* CLL LN material. Inhibition of PI3K-AKT-mTOR signaling abrogated MCL-1 upregulation and survival by Mϕs, as well as CD40 stimulation. MCL-1 can be regulated at multiple levels, and we established that AKT leads to increased MCL-1 translation, but does not affect MCL-1 transcription or protein stabilization. Furthermore, among Mϕ-secreted factors that could activate AKT, we found that induction of MCL-1 and survival critically depended on C-C motif chemokine receptor-1 (CCR1). In conclusion, this study indicates that two distinct micro-environmental factors, CD40L and Mϕs, signal via CCR1 to induce AKT activation resulting in translational stabilization of MCL-1, and hence can contribute to CLL cell survival.

Oncogene (2017) **36,** 3651–3660; doi:10.1038/onc.2016.515; published online 13 February 2017

INTRODUCTION

Chronic lymphocytic leukemia (CLL) is characterized by accumulation of monoclonal B cells in peripheral blood, lymph nodes (LNs) and the bone marrow. Interactions with bystander cells such as stromal cells, T cells or macrophages (Mϕs) in the LN provide CLL cells with a survival benefit and resistance to chemotherapy, because of changes in the apoptotic balance in CLL cells.[1] The important role of Mϕs was very recently shown in Mϕ depletion experiments in the TCL1 CLL mouse model, in which a better overall survival was observed.[2]

With respect to relevant survival factors, we have previously shown that the effects of LN-residing T cells on CLL cells are largely governed by CD40L interaction, as CLL cells stimulated by CD40L and T cells have similar gene expression and apoptotic profiles.[3] Factors from monocyte-derived nurse-like cells that have been described to induce survival include CXC motif chemokine ligand 12,[4] A proliferation-inducing ligand (APRIL) and B-cell-activating factor. These latter two factors are reported to induce nuclear factor (NF)-κB activation.[5] Using several complementary approaches, we, however, found negligible effects of APRIL in Mϕ-mediated survival,[6] implying that other Mϕ factors must be involved.

Concerning the change in apoptotic balance, our group and others have previously shown increased expression of pro-survival B-cell lymphoma 2 (BCL-2) family members in CLL cells isolated from LNs,[7] as well as in CLL cells stimulated with T-cell factor CD40L.[3,8–10] Clinically, such changes in apoptosis regulation correlate with worse prognosis and resistance to chemotherapy, as several groups have shown for pro-survival proteins BCL-2-related protein A1 (BFL-1) and BCL-extra large (BCL-X_L),[11,12] as well as induced myeloid leukemia cell differentiation protein 1 (MCL-1) levels.[13–16] The effects of monocyte-derived cells such as Mϕs on the apoptotic balance are less well studied.

The negative prognostic impact of Mϕs in CLL[2] and the fact that their extracellular and intracellular signaling events toward CLL cells are unknown, suggest that unraveling these pathways can contribute to development of new therapies. We therefore studied the effects of both Mϕs and CD40L on CLL cell survival and identified chemokine receptor CCR1 as an important mediator of Mϕ-induced CLL cell survival. Second, we found that within the CLL cell, both Mϕs and CD40L increase V-Akt murine thymoma viral oncogene homolog (AKT)-mammalian target of rapamycin (mTOR)-dependent translation of MCL-1 protein.

[1]Department of Hematology, Academic Medical Center, University of Amsterdam, Amsterdam, The Netherlands; [2]Department of Experimental Immunology, Academic Medical Center, University of Amsterdam, Amsterdam, The Netherlands; [3]Department of Hematopoiesis, Sanquin Research, Amsterdam, The Netherlands; [4]Department of Clinical Epidemiology, Biostatistics and Bioinformatics, Academic Medical Center, University of Amsterdam, Amsterdam, The Netherlands and [5]Lymphoma and Myeloma Center Amsterdam (LYMMCARE), Amsterdam, The Netherlands. Correspondence: Dr E Eldering, Department of Experimental Immunology, Academic Medical Center, University of Amsterdam, Meibergdreef 9, Amsterdam, 1105 AZ Noord-Holland, The Netherlands.
E-mail: e.eldering@amc.nl
[6]Shared senior authorship.
Received 19 October 2015; revised 5 December 2016; accepted 12 December 2016; published online 13 February 2017

RESULTS

T cells and Mϕs induce CLL survival by changing the apoptotic balance

As we have shown previously that stimulation of CLL cells via CD40 almost fully mimics the effects of activated T cells on CLL,[3] we used NIH-3T3 cells transfected with CD40L (3T40 cells) as a model for the interaction with T cells. We also generated M1 and M2 differentiated Mϕs from monocytes isolated from healthy donors by differentiation with interferon-γ (M1) or interleukin-4 (M2). Both types of Mϕs and 3T40 cells increased survival of CLL cells after 72-h co-culture (Figure 1a).

We analyzed 72-h-stimulated CLL cells for anti-apoptotic proteins MCL-1, BCL-X_L, BFL-1 and BCL-2 using western blot. MCL-1 was upregulated by both Mϕ types and 3T40 stimulation, whereas BCL-X_L and BFL-1 were only upregulated by 3T40 stimulation, consistent with activation of nuclear factor of kappa light polypeptide gene enhancer in B cells (NF-κB) by 3T40 cells[10] (Figure 1b, Supplementary Figure S1 for size markers).

To verify the relevance of MCL-1 upregulation in the observed survival effect of Mϕ, small interfering RNA (siRNA) interference using Amaxa nucleofection was applied, before co-culture on M1 Mϕs (Figure 1c). The Mϕ-mediated survival effect was largely reverted after MCL-1 knockdown. Thus, in the Mϕ setting, CLL cells depend on the upregulation of MCL-1 for their survival.

The expression of MCL-1 in CLL LNs and the presence of Mϕs were verified by immunohistochemical staining. These stainings indicated that MCL-1 is present at significant levels in LN-residing CLL cells and that the LN is interspersed with Mϕs (Figure 1d, and Supplementary Figure S2 for single channel images).

MCL-1 induction depends on PI3K-AKT-mTOR signaling after both CD40L and Mϕ stimulation

To identify which intracellular pathway was responsible for the observed MCL-1 upregulation, genome-wide expression profiling (using microarrays) of stimulated CLL cells was performed. A comparison of the log fold changes of the expression levels of each gene in stimulated cells versus the control condition showed a large overlap between regulated genes in M1 and M2-stimulated samples (Figure 2a; $R^2 = 0.72$). When comparing either M1 or M2 to 3T40-stimulated samples, there was more discordance and only limited overlap ($R^2 = 0.03$ and 0.00, respectively).

As both CD40L, M1 and M2 stimulation induced MCL-1 (Figure 1b), we hypothesized that the same upstream regulator was responsible for its induction by all stimuli. Using ingenuity pathway analysis, potential upstream regulators for each condition were determined and these upstream regulators were marked in a scatterplot (Figure 2b). Interferon-α and PI3K, the upstream regulator of the PI3K/V-Akt murine thymoma viral oncogene homolog (AKT)/mTOR pathway, were predicted to be activated in all three conditions. These data were confirmed in a CAMERA pathway analysis using the Molecular Signatures Database v5.1 (MSigDB, Broad Institute, Cambridge, MA, USA) (data not shown). Of note, neither M1 nor M2 Mϕs expressed CD40L as determined by flow cytometry (data not shown), indicating that another factor is responsible for the observed Mϕ effect. As M1 and M2-stimulated CLL cells had highly similar gene expression and functional profiles (Figures 1a and b and 2a), we used the more tightly adherent M1 Mϕs for further experiments (hereafter called Mϕ). Furthermore, considering that interferon-α is not secreted by 3T40 cells, we decided to focus on the AKT pathway activation.

In accordance with the microarray data, we found that both 3T40 and Mϕs induced AKT phosphorylation (Figure 2c). To test for sustained functional activation of AKT, phosphorylation of its downstream target GKS3β[17] was probed after 6h, showing phosphorylation after both stimuli (Figure 2d). The phosphorylation of GKS3β was furthermore found in FACS-sorted CLL cells from LN material, indicating active AKT signaling *in vivo* (Supplementary Figure S3).

To test whether MCL-1 induction depended on AKT-mTOR signaling, we used two pharmacological inhibitors of mTOR; AZD8055, which competes for the ATP binding pocket[18] and the allosteric inhibitor rapamycin.[19] Both inhibitors were able to completely revert the CLL survival effect conferred by Mφs. However, they did not revert CD40-induced survival, likely due to the concurrent upregulation of anti-apoptotic proteins BFL-1 and BCL-X_L. AZD8055 reduced MCL-1 levels in both Mφ and 3T40-stimulated CLL cells. Rapamycin on the other hand showed only an effect in CD40L-stimulated CLL cells (Figure 2e). Rapamycin, as opposed to AZD8055, is unable to inhibit the mTORC2-mediated positive feedback loop[19,20] and mTOR-mediated eukaryotic translation initiation factor 4E-binding protein (4E-BP) phosphorylation has been shown to be resistant to rapamycin treatment.[20] Next, CAL101 (idelalisib), which inhibits PI3Kδ, was used to decrease AKT activation.[21] Idelalisib treatment showed a reduction in MCL-1 protein for both conditions, but only reduced Mφ-mediated (and not 3T40-mediated) CLL survival (Figure 2f).

Collectively, these data suggest that the observed induction of MCL-1 after CD40L or Mφ stimulation depends on PI3K-AKT-mTOR signaling.

MCL-1 is induced on the translational level

Protein stabilization via AKT-dependent glycogen synthase kinase 3β (GSK3β) phosphorylation has been attributed an important role in MCL-1 induction.[22–24] We therefore measured MCL-1 turnover after addition of translation inhibitor cycloheximide. However, these analyses indicated similar stability of MCL-1 protein before and after co-culture with Mφ or 3T40 cells (Figure 3a). Furthermore, treatment with CHIR99021, a selective GSK3 inhibitor, induced no changes in MCL-1 half-life, while the upregulation of β-catenin, another GSK3β substrate, indicated effective GSK3β inhibition (Figure 3b).

As AKT is furthermore involved in the formation of the translation initiation complex, we evaluated changes in translation of *MCL-1* mRNA, by measuring the amount of mRNA bound in actively translating ribosome chains, or polysomes. Sucrose gradient centrifugation of cell lysates was used[25] to separate polysomal and non-polysomal mRNA and determine the fraction of polysomal *MCL-1* mRNA. These analyses showed an increase in polysomal bound *MCL-1* mRNA of approximately 2-fold in 3T40 and 3.5-fold in Mφ-stimulated samples, indicating an increase in *MCL-1* mRNA translation. The distribution of *18S* ribosomal RNA, in contrast, was not altered upon exposure to 3T40 cells or Mφs, implying that the number of actively translating ribosomes did not change (Figure 3c and Supplementary Figure S4a for a representative BioAnalyzer profile).

The formation of polysomes is initiated after the phosphorylation of several translation initiation factors that are part of the eukaryotic translation initiation factor 4 (eIF4) complex.[26] Association of this complex with mRNA depends on the cap-binding factor eIF4E, which is inhibited by 4E-BP. The mTOR-dependent phosphorylation of 4E-BP releases eIF4E to increase translation initiation,[27] while extracellular signal-regulated kinase (ERK)-dependent phosphorylation of eIF4E enhances formation of the eIF4 complex.[28] Furthermore, the phosphorylation of ribosomal protein S6, which is part of the 40S ribosome, has been implicated in translation initiation.[29] Thus, the phosphorylation of eIF4E, 4E-BP and S6 correlate with an increase in translation.[27]

We therefore analyzed the phosphorylation status of these proteins and found that stimulation with either Mφs or 3T40 cells consistently resulted in upregulation of phosphorylation of 4E-BP and S6. Moreover, 3T40 stimulation also increased eIF4E phosphorylation (Figure 3d). In accordance, ERK was

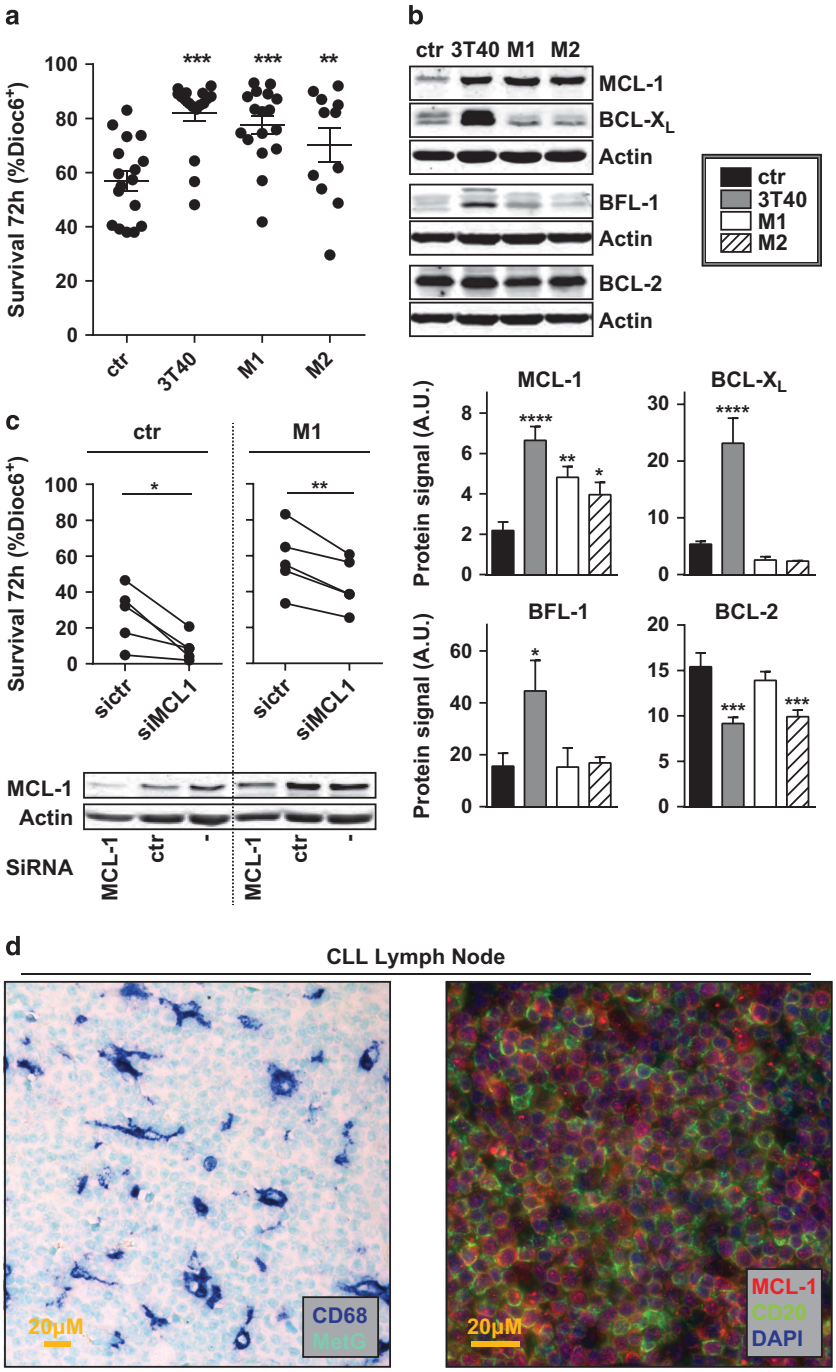

Figure 1. Mϕs and CD40L induce CLL survival by changing the apoptotic balance. Confluent feeder layers of Mϕs and non-dividing CD40L-overexpressing fibroblasts (3T40) were generated as described under Materials and methods section. (**a**) CLL cells were co-cultured on the indicated feeder layers or without feeder layer (ctr) for 72 h after which survival was measured by Dioc6-PI staining. The percentage of viable cells was defined as Dioc6-positive cells. Each point represents one stimulation of a CLL sample. Shown are mean ± s.e.m. (**b**) After 72-h co-culture as in **a**, protein lysates of CLL cells were probed by western blot for the levels of pro-survival BCL-2 family members MCL-1, BCL-X_L, BFL-1 and BCL-2. β-Actin was used as a loading control. Data shown are representative of at least $N = 6$. To improve clarity, western blot images were cropped in this and following figures (upper panel). The levels of each protein were quantified for six patients using densitometry and calculated as the protein signal relative to the actin loading control (lower panel). A.U. denotes arbitrary units. (**c**) CLL cells were transfected with one of two siRNAs directed against *MCL-1* (siMCL-1) or a control (sictr) or not transfected (−) before co-culture on Mϕs or without feeder layer (ctr). After 72 h, the viability of CLL cells was determined as in **a**. Each line represents one patient sample. Transfection efficiency using a green fluorescent protein control plasmid has previously been determined to be approximately 50% (data not shown) (upper panel). Protein lysates of CLL cells were probed for MCL-1 levels by western blot to verify the knockdown. β-Actin was used as a loading control. Data shown are representative of $N = 5$ (lower panel). (**d**) Paraffin-embedded LN slides from CLL patients were immunohistochemically stained for Mϕ marker CD68 and nuclear counterstain methyl green (left panel), or MCL-1, B-cell marker CD20 and nuclear counterstain 4,6-diamidino-2-phenylindole (DAPI; right panel). Data shown are representative of $N = 6$. *$P < 0.05$; **$P < 0.01$; ***$P < 0.001$; ****$P < 0.0001$ in an analysis of variance (ANOVA) test with Dunnett's post-hoc test (**a**, **b**) or in a *t* test (**c**).

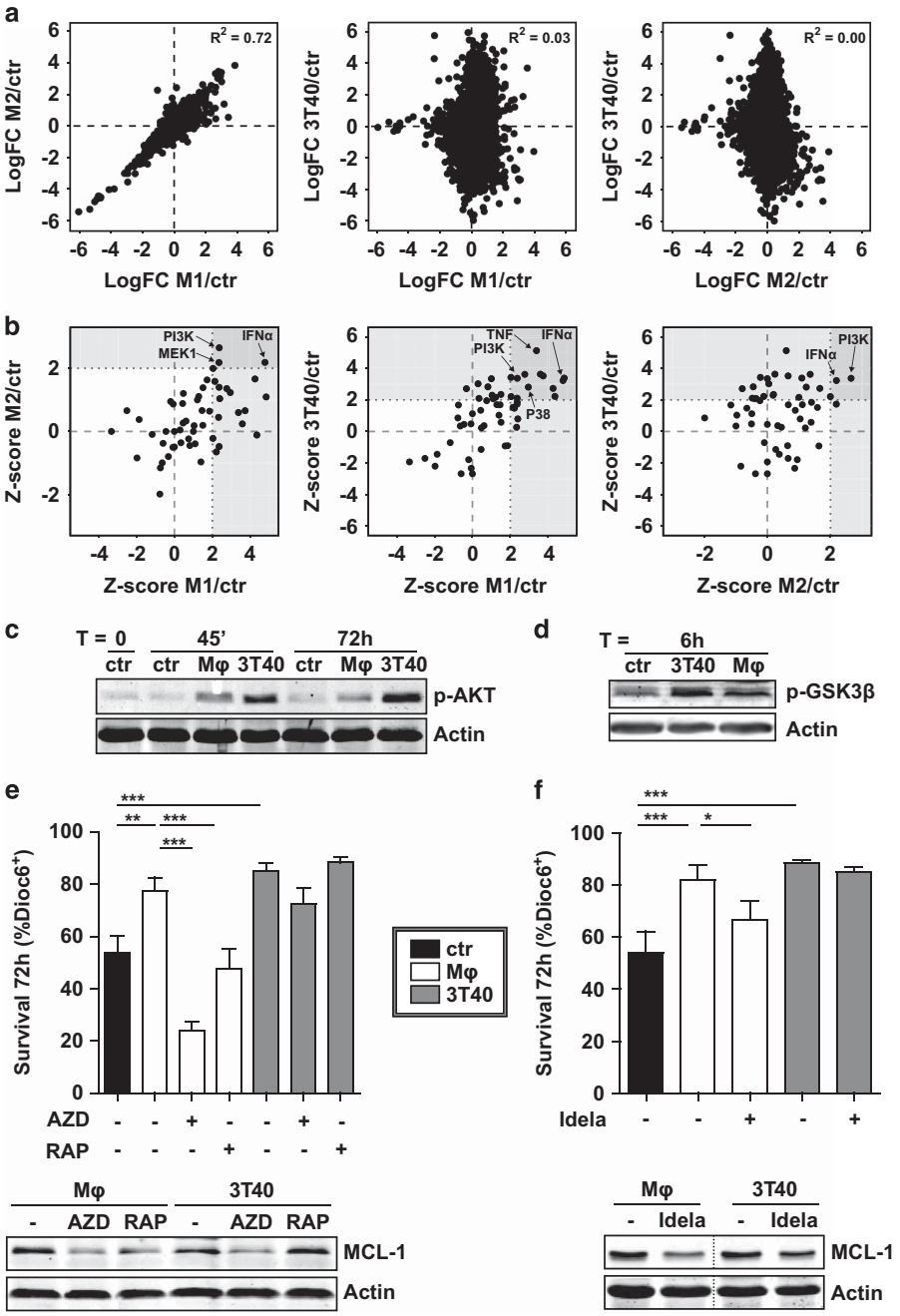

Figure 2. MCL-1 induction depends on PI3K-AKT-mTOR signaling after both CD40L and Mϕ stimulation. (**a**) CLL cells were co-cultured as in Figure 1 ($N=3$ paired samples for each condition) for 16h and RNA from CD5/CD19 FACS-sorted CLL cells (>99% purity) was subjected to microarray analysis. Next, for each mRNA, the log fold change (LogFC) relative to control condition was calculated and plotted. The goodness of fit for the linear regression models (R^2) is indicated. (**b**) A core analysis in the ingenuity pathway analysis (IPA) software was performed with signatures created from the microarray data based on cut-off values logFC >0.8 and *P*-value <0.01 to identify putative upstream regulators common to all three stimuli. The *Z*-score of candidate upstream regulators was visualized in scatterplots, in which upstream regulators with a *Z*-score over 2.0 were defined as activated, in line with IPA specifications. Several potentially relevant activated regulators are indicated by arrows. (**c**) CLL cells were serum starved for 3 h and subsequently co-cultured as in Figure 1 on indicated feeder layers for indicated time points and the phosphorylation of AKT was determined by western blot (shown blot is representative of $N=4$). β-Actin was used as a loading control. (**d**) After resting for 3 h, CLL samples were co-cultured as in Figure 1 on indicated feeder layers for 6h and the activation of AKT signaling was determined by western blotting for phosphorylated GSK3β (blot representative of $N=4$). (**e**) CLL samples were co-cultured as in Figure 1 in the presence or absence of mTOR inhibitors AZD8055 (500nM) or rapamycin (1μM) and survival was determined as in Figure 1a. Shown are mean ± s.e.m. for $N=9$ (untreated and RAPA) or $N=3$ (AZD) samples (upper panel). Similarly treated CLL samples were subjected to western blot and probed for MCL-1. To exclude caspase-mediated MCL-1 breakdown, 5μM Q-VD-OPh was added to all samples during culture when analyzed for MCL-1 levels by western blotting. β-Actin was used as a loading control. Western blot representative for $N=6$ (lower panel). (**f**) CLL samples were co-cultured as in Figure 1 in the presence or absence of 1μM PI3K inhibitor CAL101 (idelalisib) and survival was determined as in Figure 1a. Shown are mean ± s.e.m. for $N=7$ (upper panel). Similarly treated CLL samples were subjected to western blot and probed for MCL-1, as in **e**. Western blot representative for $N=4$. *$P<0.05$; **$P<0.01$; ***$P<0.001$ in an ANOVA test with Newman-Keuls post-hoc test (**e**, **f**).

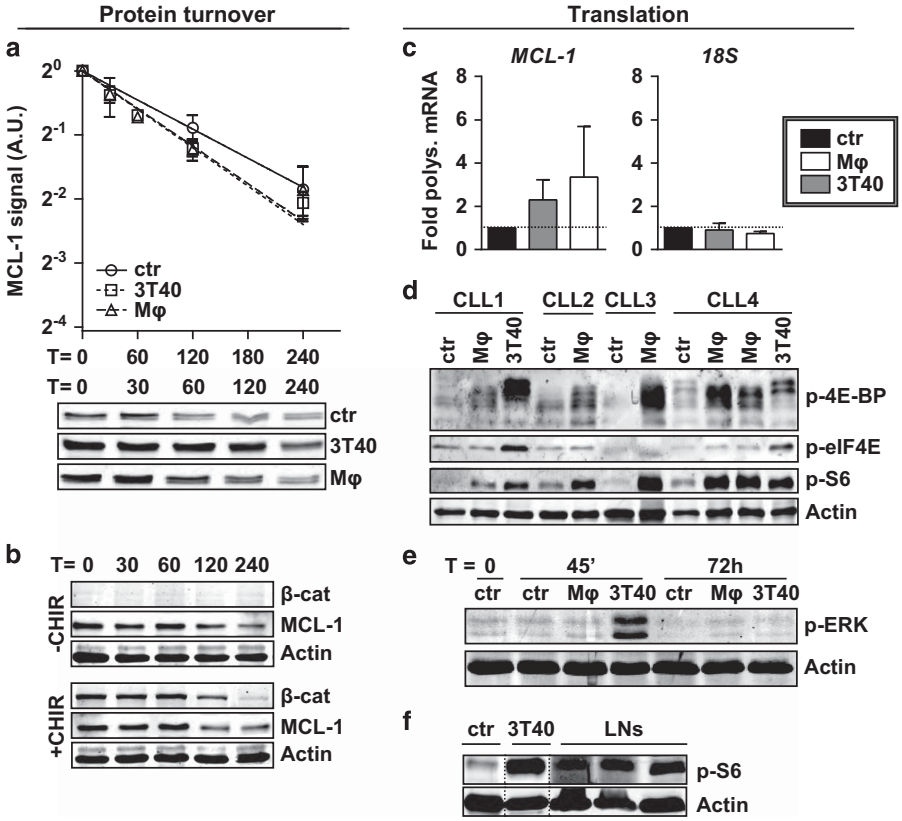

Figure 3. MCL-1 is regulated on translational level. (**a**) After co-culture for 72 h, turnover of MCL-1 in CLL cells was determined by quantifying levels at different time points after addition of 25 μg/ml translation inhibitor cycloheximide, and compared with unstimulated samples ($N=6$). Each point represents mean ± s.e.m. and regression lines were calculated using a best-fit exponential decay model fitted with the formula $Y=Y0*e^{k*X,}$ in which Y0 was set to 1. The best-fit k value was not significantly different between lines (upper panel). A representative turnover western blot for 1 CLL sample is shown (lower panel). Note the higher MCL-1 starting levels in the stimulated samples. A.U. denotes arbitrary units. (**b**) Unstimulated CLL samples were pre-treated or not treated for 1 h with 3 μM GSK3 inhibitor CHIR99021 before MCL-1 turnover was determined as in **a**. To exclude caspase-mediated MCL-1 breakdown, 5 μM Q-VD-OPh was added to all samples during culture when analyzed for MCL-1 levels by western blotting. A representative CLL sample of $N=3$ is shown. (**c**) The translational efficiency of *MCL-1* mRNA was determined after 48 h co-culture by calculating the percentage of *MCL-1* mRNA bound in polysomes, by performing qPCR on sucrose gradient-separated non-polysomal and polysomal fractions (see Materials and methods section and Supplementary Figure S4a). An *MCL-1* and *18S* qPCR were performed on pooled samples (polysomal/non-polysomal) and the relative amount of polysomal bound mRNA ± s.e.m. ($N=4$ independent experiments) compared with the control condition (fold induction) was calculated for *MCL-1* or *18S* RNA. (**d**) CLL samples used in Figure 1b were again subjected to western blot and probed for phosphorylation of translation initiation factors and phosphorylation of ribosomal protein S6, the latter is indicative of active translation. β-Actin was used as a loading control. Note that although the anti-p-4E-BP antibody was expected to detect only the slowest migrating form of 4E-BP, the non- and partially phosphorylated forms are also detected, most likely due to cross-reactivity to the unphosphorylated site. (**e**) The western blot presented in Figure 2c was probed for ERK phosphorylation (shown blot is representative of $N=4$). (**f**) Protein lysates from three CLL LN samples were analyzed by western blot for the phosphorylation of ribosomal protein S6 as a measure for active translation. An unmatched unstimulated and 3T40-stimulated CLL sample were included for comparison.

phosphorylated exclusively by 3T40 and not by Mφs (Figure 3e). As PIM1 and PIM2 kinases have also been described to correlate with 4E-BP phosphorylation,[30] we analyzed their expression levels, but found no difference in either *PIM1* or *PIM2* expression upon stimulation (Supplementary Figure S4b).

Finally, we used protein lysates from FACS-sorted CLL cells isolated from LNs to investigate whether translation was activated *in vivo* and found phosphorylated S6 in all investigated LNs (Figure 3f). Owing to a high background signal in the CLL LN lysates, we were unable to detect p-4E-BP (data not shown). The upregulation of MCL-1 in CLL on the same LN samples was previously shown by our group.[7]

In line with our findings of translational stabilization, we found no transcriptional induction of *MCL-1* when analyzing the microarray data sets generated for Figure 2 by any stimulation, in contrast to *BCL-X$_L$* and *BFL-1*, known targets of NF-κB (Supplementary Figure S4c). In agreement, after Mφ co-culture, no NF-κB subunit translocation occurred (Supplementary Figure S4d), and no NF-κB DNA binding activity could be detected in CLL cells using enzyme-linked immunosorbent assay (Supplementary Figure S4e).

In summary, 3T40 cells nor Mφs to transcriptional upregulation or post-translational stabilization of MCL-1, but both stimuli induced translation of *MCL-1* mRNA by activation of the initiation complex. This translational activation signature was also present in *ex vivo* LN samples.

MCL-1 upregulation and CLL cell survival are CCR1-dependent

We then aimed to identify the Mφ-produced factor responsible for the observed survival increase and MCL-1 upregulation via AKT. Various Mφ-secreted factors have been described to induce AKT signaling, among which are growth factors,[31,32] integrin signals[33] and chemokines.[34] As trans-well culturing experiments showed Mφ-mediated survival in the non-contact setting (Supplementary

Figure S5), we focused on soluble factors for their ability to induce CLL cell survival, while not excluding contact-dependent factors. Using several recombinant growth factors, we could not recapitulate the Mφ survival effect (Figure 4a). To test the effect of integrin signaling, CLL cells were cultured on plates pre-coated with fibronectin or VCAM, which stimulate several integrin receptors.[35] As integrin signaling has been described to affect growth factor signaling,[36] these stimulations were performed with or without a combination of the growth factors used in Figure 4a. Again, none of these stimuli induced survival in CLL cells (Figure 4b). Furthermore, inhibition of integrin signaling in Mφ-stimulated samples did not affect survival (data not shown). Finally, highly specific chemokine inhibitors for CCR1, CCR2 and CCR5 were tested in the context of Mφ-stimulated CLL cells. Of

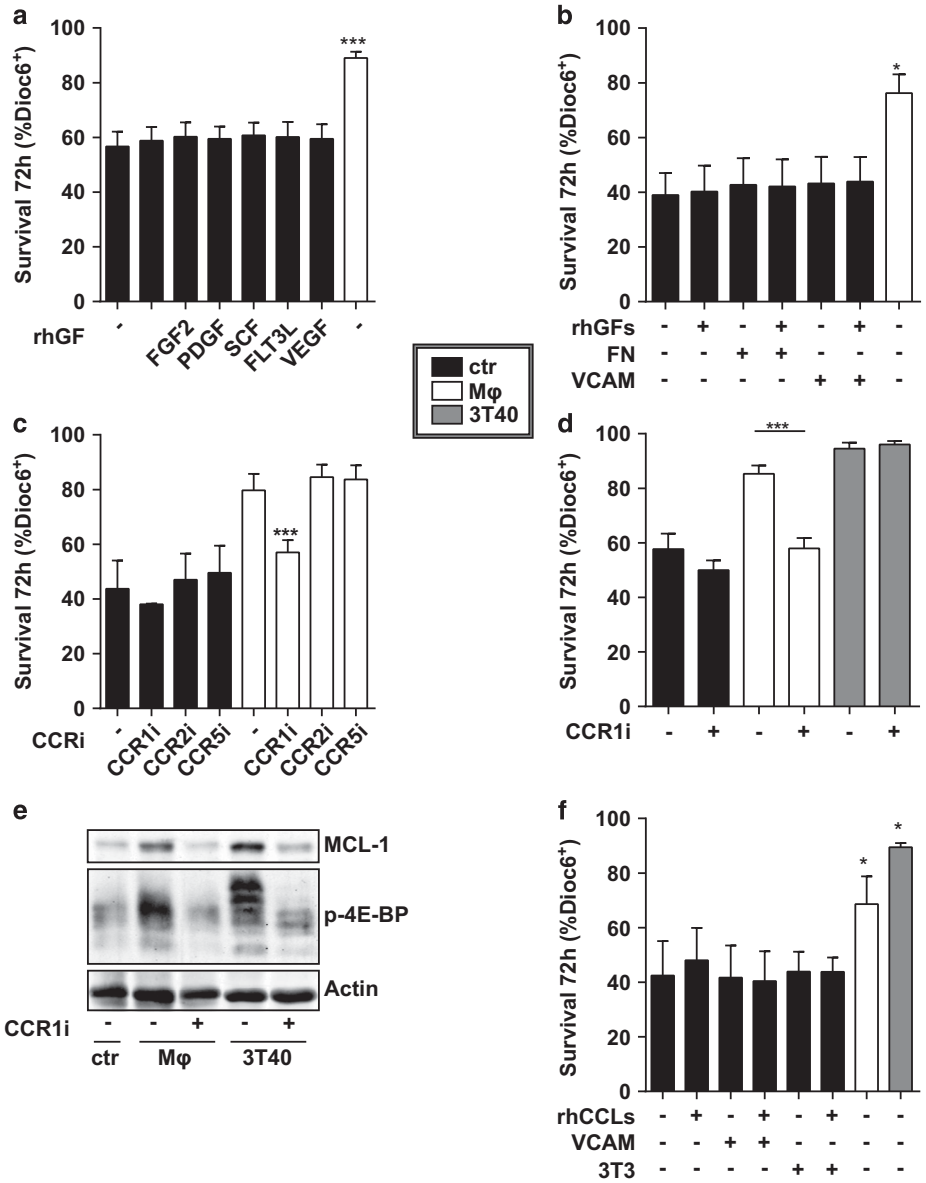

Figure 4. MCL-1 upregulation and CLL cell survival are CCR1 dependent. (**a**) CLL samples were cultured in the presence of 25 ng/ml epidermal growth factor (EGF), 20 ng/ml basic fibroblast growth factor (FGF2), 10 ng/ml platelet-derived growth factor (PDGF), 50 ng/mll stem cell factor (SCF), 25 ng/ml Fms-related tyrosine kinase 3 ligand (FLT3L), 10 ng/ml vascular endothelial growth factor (VEGF), or nothing or on Mφ for 72 h and survival was measured. Shown are mean ± s.e.m. for $N = 6$ CLL samples. (**b**) CLL cells were cultured without feeder layer, or on fibronectin coated plates (FN), on VCAM-coated plates (VCAM) or on Mφ for 72 h in the presence of absence of a combination of the growth factors (rhGFs) used in Figure 5a. Survival is shown as mean ± s.e.m. for $N = 3$ CLL samples. (**c**) CLL cells were co-cultured on Mφ or without feeder layer (ctr) for 72 h in the presence of absence of specific CCR inhibitors against CCR1 (1 μg/ml BX471), CCR2 (100 ng/ml INCB3284) or CCR5 (1 μM Maraviroc). Next, survival was measured as in Figure 1a. Shown are mean ± s.e.m. for $N = 3$ CLL samples. (**d**) CLL cells were co-cultured on indicated feeder layers or without feeder layer (ctr) for 72 h in the presence of absence of CCR1 inhibitor BX471. Next, survival was measured as in Figure 1a. Shown are mean ± s.e.m. for $N = 9$ CLL samples. (**e**) After 72 h co-culture as in Figure 3d, protein lysates of CLL cells were probed by western blot for MCL-1 and p-4E-BP. Note that the smear for p-4E-BP in the Mφ sample could result from differently phosphorylated 4E-BP forms. Data shown for one patient are representative of $N = 3$. (**f**) CLL cells were co-cultured on indicated feeder layers for 72 h or cultured with a combination of CCR1-binding chemokines CCL3, 5 and 23 on non-coated or VCAM-coated plates or on 3T3 cells. Next, survival was measured as in Figure 1a. Shown are mean ± s.e.m. for $N = 3$ CLL samples comparing each feeder layer with to without chemokines or Mφ or 3T40 to control. $^*P < 0.05$; $^{***}P < 0.001$ in an ANOVA test with Dunnett's (**a**, **b**, **f**) or Newman-Keuls (**c**, **d**) post-hoc test.

these, inhibition of only CCR1 lead to a complete abrogation of the Mφ-induced survival effect (Figure 4c). This survival reduction was not the result of nonspecific cytotoxic effects, as unstimulated cell survival was not affected by CCR1 inhibition. We verified the effect of CCR1 inhibition in nine CLL samples, and moreover included 3T40-stimulated CLL cells. Again, CCR1 inhibition completely negated the Mφ-mediated CLL cell survival, whereas it had no effect on 3T40-mediated survival (Figure 4d). The absence of an effect in the context of 3T40 stimulation likely results from the concurrent upregulation of BCL-X_L and BFL-1 after 3T40 stimulation (Figure 1b).

We then investigated whether the reduction in survival was mediated via MCL-1 and found that in both Mφ and 3T40-stimulated CLL cells, CCR1 inhibition led to a strong reduction in MCL-1 protein levels. In addition, the phosphorylation of 4E-BP was reduced after CCR1 inhibition, indicating involvement of AKT-mTOR signaling in CCR1-mediated MCL-1 induction (Figure 4e).

As several chemokine ligands have been described to signal via CCR1,[37] we tested if a combination of rhCCL3, CCL5 and CCL23 could mimic the Mφ survival effect. As chemokine signaling can be dependent on presentation via heparin sulfate proteoglycans, these experiments were also performed using feeder layers of VCAM or NIH-3T3 cells, which express heparin sulfate proteoglycans. However, no survival benefit of the recombinant proteins was observed (Figure 4f), suggesting that the relevant chemokine acts in conjunction with a second Mφ-secreted factor.

Altogether, these data indicate a dependence on CCR1 in both both Mφ- and CD40L-mediated survival.

DISCUSSION

In this article, we investigated how two important micro-environmental signals, CD40L and Mφs, lead to upregulation of key anti-apoptotic protein MCL-1 in primary leukemic cells, studying both extracellular and intracellular factors. In contrast to our starting assumption that MCL-1 in CLL cells is mostly post-translationally regulated, we determined that both Mφ and CD40L stimulation induced MCL-1 via AKT-dependent activation of the translation initiation complex (Figure 5). Several observations support the notion that activation of the initiation complex results in a specific translational increase of MCL-1. First, mRNAs with long GC-rich highly structured 5′ untranslated regions, such as the mRNA from MCL-1, are particularly sensitive to translational regulation.[38] Second, in the Tsc2(+/−)Eμ-Myc mouse model, which has constitutive mTORC1 activation, translationally induced Mcl-1 appeared to be the main determinant of survival.[39] Third, the survival effect that resulted from expression of constitutively active AKT (myr-AKT) in CLL cells, could be reverted by down-regulation of MCL-1 by siRNAs.[40] Fourth, overexpression of a phosphomimetic S209D eIF4E variant in cancer cell lines selectively increases the translation of a limited number of proteins, among which is MCL-1.[41] Fifth, inhibition of the translation complex following glucose deprivation sensitizes cells to death receptor-mediated apoptosis as a result of translational MCL-1 downregulation.[42] Modification(s) of translation factors could thus be a micro-environmental regulatory mechanism inducing specifically pro-survival proteins such as MCL-1.

In addition to translational control, several reports describe post-translational stabilization of MCL-1 that is mediated via GSK3β.[22,24] Other reports show an increase in MCL-1 transcription in CLL after co-culture with mesenchymal stromal cells,[43] or after signal transducer and activator of transcription activation with cytokines.[44] Our observation of translational regulation of MCL-1 independent of GSK3β adds to the wide spectrum of MCL-1 control. These distinct mechanisms of MCL-1 control are not mutually exclusive and their relevance will probably depend on the cellular context, and apparently post-translational stabilization is not the dominant mechanism in primary CLL cells.

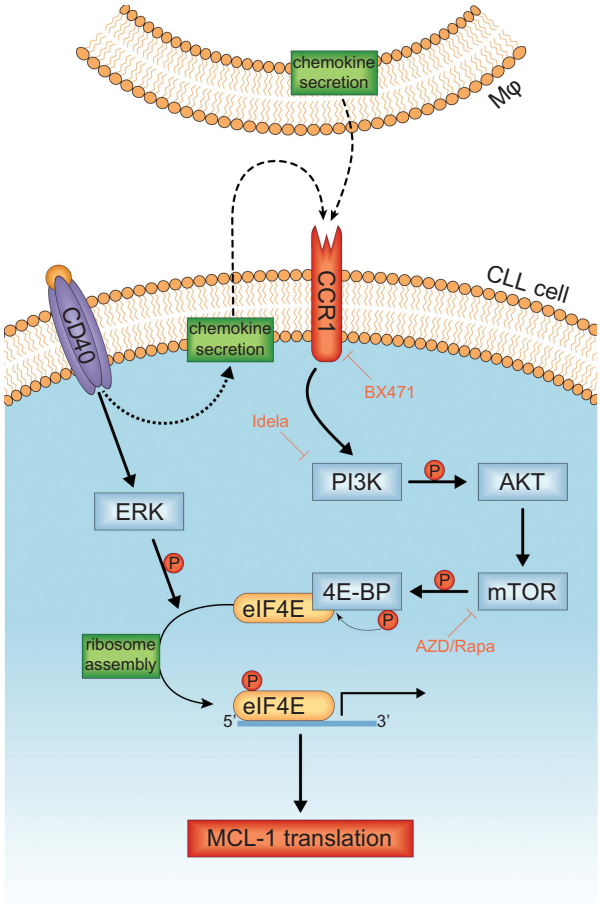

Figure 5. Schematic model for the chemokine-mediated micro-environmental translational regulation of MCL-1. Chemokines secreted directly by Mφs or in an autocrine fashion by CLL cells after CD40 stimulation lead to triggering of the CCR1 receptor. This triggering induces AKT signaling and subsequent induction of mTOR-dependent 4E-BP phosphorylation and release of its inhibited binding partner eIF4E. Concurrently, the induction of ERK signaling by CD40 stimulation results in the phosphorylation of eIF4E. These processes facilitate the recruitment of eIF4E to the 5′ mRNA cap and formation of the ribosome, which results in the active translation of mRNA of pro-survival proteins like MCL-1.

Furthermore, MCL-1 upregulation after CD40L or Mφ stimulation was independent of NF-κB activation (Supplementary Figures S4d–e). In agreement, no consensus NF-κB-binding sites can be found in the *MCL-1* promotor (Supplementary Figure S4f). Although several publications report a correlation between NF-κB activation and MCL-1 levels in CLL cells in response to other stimuli,[5,44,45] this may very well be due to autocrine interleukin-mediated MCL-1 upregulating signals that respond to NF-κB activation,[44] or alternatively, MCL-1 and NF-κB are both regulated by an upstream activator, as is the case for CD40 signals. In summary, it appears that under certain conditions NF-κB activation can indirectly induce *MCL-1* transcription.

We have found that the responsible Mφ factor for CLL survival is a chemokine that signals via CCR1, while excluding growth factors, and integrins. In this light, we have moreover excluded the involvement of A proliferation-inducing ligand (APRIL)[6] and CD40L (data not shown). Chemokines that can signal via CCR1 include CCL3, 4, 5, 7, 14, 15, 16 and 23.[37] Interestingly, the reduction in MCL-1 levels after CCR1 inhibition of 3T40-stimulated CLL samples suggests that this upregulation of MCL-1 depends on (indirect)

chemokine-mediated signals. Indeed, we recently observed production of several chemokines such as CCL3, 5 and 7 by CLL cells after 3T40 stimulation (Van Attekum *et al.*, manuscript in revision), in support of a model in which MCL-1 upregulation after 3T40 stimulation depends on autocrine chemokine stimulation of CLL cells (Figure 5).

In conclusion, our data indicate that two model systems of important micro-environmental stimuli (CD40L and Mφs) are able to induce survival in primary CLL cells by upregulating MCL-1 translation via AKT signaling. This MCL-1 upregulation resulted from CCR1-mediated signals after both stimuli. These insights may be applicable in designing new treatment strategies for CLL.

MATERIALS AND METHODS

CLL and healthy donor material and isolation

Patient material was obtained from CLL patients, after written informed consent, during routine follow-up or diagnostic procedures at the Academic Medical Center, Amsterdam, The Netherlands. The studies were approved by our ethical review board and conducted in agreement with the Helsinki Declaration of 1975, revised in 1983. Peripheral blood mononuclear cells of CLL patients were isolated using ficoll (Pharmacia Biotech, Roosendaal, The Netherlands) and stored in liquid nitrogen. Expression of CD5 and CD19 (both Beckton Dickinson Biosciences (BD), San Jose, CA, USA) on leukemic cells was assessed by flow cytometry (FACS Canto, BD) and analyzed with FACSDiva software (BD). All samples contained at least 90% $CD5^+/CD19^+$. More information on the characteristics of the CLL patients that provided material can be found in Supplementary Table 1.

Monocyte-derived Mφs were obtained by differentiating monocytes isolated from healthy donor buffy coats after obtaining written informed consent. To this end, peripheral blood mononuclear cells were isolated using ficoll gradient purification according to the manufacturer's instructions (Lucron, Dieren, The Netherlands), after which monocytes were separated from peripheral blood lymphocytes using percoll gradient purification (GE Healthcare, Milwaukee, WI, USA). Next, monocytes were incubated to adhere at 37 °C in 5% CO_2 for 40 min at a concentration of 0.75×10^6 cells/ml in six-well plates (3 ml) in iscove's modified dulbecco's medium (IMDM)/1% fetal bovine serum (Invitrogen, Carlsbad, CA, USA) and washed to remove non-adherent cells. The monocytes were then differentiated to either M1 using 10 ng/ml IFN-γ or M2 using 10 ng/ml interleukin-4 (both R&D Systems, Minneapolis, MN, USA) in IMDM supplemented with 10% fetal bovine serum, 100 u/ml penicillin-100 µg/ml streptomycin (Life Technologies, Austin, TX, USA), 2 mM L-glutamine (Life Technologies) and 0.00036% β-mercaptoethanol (Sigma, St Louis, MO, USA; $IMDM^{+/+}$) for 72 h.

Cell culture and co-culture experiments

NIH-3T3 mouse embryo fibroblasts (3T3 cells) were supplied and characterized (for identity control, cytogenetics and immunophenotype) by the Deutsche Sammlung von Mikroorganismen und Zellkulturen GmbH (DSMZ, Braunschweig, Germany). To mimic T-cell-induced CD40 signaling, these 3T3 cells were stably transfected with human CD40L (3T40 cells) as described previously.[8] When used as adherent feeder layer, fibroblasts were irradiated (30Gy) to stop proliferation before being seeded. Mφs were created as described under 'CLL and healthy donor material and isolation'. After differentiation, Mφs were washed twice with $IMDM^{+/+}$. CLL samples were thawed and diluted to a concentration of 1.5×10^6 cells/ml before being plated on the respective feeder cells and co-cultured for indicated times. Trans-well experiments were performed according to the manufacturer's instructions using 0.4 µm pore size 24-well culture plates (Corning, Corning, NY, USA).

Microarrays and bioinformatic analyses

CLL samples were stimulated with Mφs or not stimulated as described under 'Cell culture and co-culture experiments'. Total RNA from these stimulated samples was prepared and microarray experiments were performed as they were for 3T40/non-stimulated samples as described before.[3] In short, RNA was isolated using TriReagent (Sigma) according to the manufacturer's instruction and RNA was further purified using the RNeasy micro kit (Qiagen, Valencia, CA, USA) according to the manufacturer's instruction including a DNAse (Qiagen) treatment. RNA was then hybridized on a U133plus2 microarray chip (Affymetrix, Santa Clara, CA, USA). The Mφ and 3T40 experiments were analyzed separately using Bioconductor packages (https://www.bioconductor.org) in the statistical software package R (version 3.1.2, R Project, Vienna, Austria). Raw data were extracted from the CEL files using the package affy (https://cran.r-project.org/). Data were normalized and summarized at the probeset level using robust multiarray averaging with default settings (function rma, package affy). Differential expression between the experimental conditions was assessed with a moderated *t*-test using the linear model framework including patient as a blocking variable (limma package, https://cran.r-project.org/). Resulting *P*-values were corrected for multiple testing using the Benjamini–Hochberg false discovery rate. Corrected *P*-values $\leqslant 0.05$ were considered statistically significant. Probes were reannotated using the Bioconductor hgu133plus2.db package. Data were visualized using the ggplot2 package (https://cran.r-project.org/). To identify upstream regulators, these differentially regulated genes were used for an Ingenuity pathway analysis using cut-off values of log fold change >0.8 and *P*-value <0.01 to select relevant regulated genes. For the CAMERA analysis, gene sets were retrieved from MSigDB v5.1 (Hallmark collection, Entrez Gene ID version): http://www.broadinstitute.org/gsea/msigdb/index.jsp and probe sets that mapped to two or more Entrez Gene IDs were excluded. Next, enrichment analysis was performed using CAMERA with preset value of 0.01 for the inter-gene correlation. The identification of NF-κB consensus sites was performed using a Python 3 script (Supplementary script).

Measurement of levels of polysomal bound *MCL-1* mRNA

In all, 40×10^6 CLL cells were co-cultured for 48 h on Mφs or 3T40 cells or left unstimulated as described under 'Cell culture and co-culture experiments'. Cells were then lysed in 1 ml NP-40 buffer (0.5% NP-40, 10 mM TrisHCl pH 8.0, 140 mM NaCl, 1.5 mM $MgCl_2$) freshly added DTT (Sigma D0632, 20 mM), cycloheximide (Sigma C7698, 150 ng/ml), RNAsin (Promega N2515, Madison, WI, USA, 12 µl/ml), and protease inhibitors (Calbiochem 539131, San Diego, CA, USA, 1:100). Lysates were loaded on linear 40–15% sucrose gradients and centrifuged for 120 min at 38 000 r.p.m. Gradients were subsequently separated in 18 fractions and each fraction was incubated for 30 min at 37 °C with 1% sodium dodecyl sulfate, 10 mM EDTA and 150 µg/ml proteinase K (Roche), after which RNA was isolated from each fraction using phenol–chloroform extraction. To identify the presence of polysomes, 1µl of each fraction was run on a 2100 Bioanalyzer (Agilent Technologies, Santa Clara, CA, USA). Non-polysomal and polysomal fractions were pooled and equal amounts of RNA were used for complementary DNA synthesis by reverse transcriptase reaction according to the manufacturer's instructions (Promega). The complementary DNA was subsequently used as input for a real-time PCR using SYBR green (Life Technologies) reaction (40 cycles of 3 s at 95 °C followed by 30 s at 60 °C), using the following primers: *MCL-1* 5′-TCGTAAGGACA AAACGGGAC-3′ and 5′-CATTCCTGATGCCACCTTCT-3′, *18S* 5′-CGGCTACCAC ATCCAAGGAA-3′ and 5′-GCTGGAATTACCGCGGCT-3′. The abundance of each RNA was then calculated using the formula

$$\%\ polysomal\ RNA = \frac{(2^{\wedge} - (\mathrm{CtHF} - \mathrm{CtLF})/(\text{input HF}/\text{input LF}))}{(2^{\wedge} - (\mathrm{CtHF} - \mathrm{CtLF})/(\text{input HF}/\text{input LF})) + 1} * 100\%$$

where Ct = Ct value of HF = heavy (polysomal) fraction and LF = light (non-polysomal) fraction and input = the volume of RNA solution used for complementary DNA synthesis. The abundance of polysomal RNA was then plotted relative to the unstimulated condition.

Reagents

Recombinant human proteins were obtained from the following the manufacturers: basic fibroblast growth factor, platelet-derived growth factor, Fms-related tyrosine kinase 3 ligand and vascular endothelial growth factor (all R&D Systems), Epidermal growth factor (Sigma), stem cell factor (Peprotech, Rocky Hill, NJ, USA), CCL3 (R&D Systems), CCL5 (R&D Systems) and CCL23 (BioLegend, San Diego, CA, USA).

The following inhibitors were used: mTOR inhibitors AZD8055 (Selleckchem, Houston, TX, USA) and rapamycin (Cell Signaling, Boston, MA, USA), PI3K inhibitor CAL101 (Selleckchem), caspase inhibitor Q-VD-OPh (Apexbio, Houston, TX, USA), GSK3 inhibitor CHIR99021 (Sigma), CCR1 inhibitor BX471 (Sigma), CCR2 inhibitor INCB3284 (Tocris Bioscience, Bristol, UK) and CCR5 inhibitor Maraviroc (Apexbio).

Cell viability assays

To assess cell viability, 100 µl of CLL cell suspension was incubated with 0.01 µM dihexyloxacarbocyanine iodide (Dioc6, Molecular Probes, Waltham, MA, USA) for 30–40 min at 37 °C. Before analysis, propidium iodide (PI, Sigma) was added (final concentration 2 µg/ml). Signals were measured on a FACS Calibur (BD) and analyzed using FlowJo software (TreeStar, San Carlos, CA, USA). Viable cells were defined as being Dioc6+/PI−.

Histology and immunofluorescence

Paraffin-embedded tissue was obtained from our institute's pathology department. Four-micron sections were de-waxed by immersion in xylene and hydrated by serial immersion in ethanol and phosphate-buffered saline (PBS). Antigen retrieval was performed by heating sections for 20 min in sodium citrate buffer (10 mM sodium citrate, 0.05% Tween20, pH 6.0). Sections were washed with PBS (2 × 10 min) and blocking buffer (Tris-buffered saline containing 10% bovine serum albumin and 0.3% Triton X-100) was added for 1 h. Sections were incubated with primary antibody, anti-CD20 (1:500, eBioscience, San Diego, CA, USA) and anti-MCL-1 (1:150, Abcam, Cambridge, MA, USA) or CD68 (Biolegend Y1-82A) in blocking buffer overnight at 4 °C. Subsequently, the slides were washed with PBS (2 × 10 min) and incubated with Alexa Fluor 488-labeled goat anti-mouse, Alexa Fluor 594-labeled goat anti-rabbit antibodies (1:400, Invitrogen) for 1 h, after which the slides were stained for 10 min with 4,6-diamidino-2-phenylindole (0.1 µg/ml in PBS). Alternatively, CD68 was developed using the VECTOR Blue Alkaline Phosphatase (AP) Substrate Kit (VectorLabs, Burlingame, CA, USA) and counterstained with methyl Green. Sections were mounted with Fluoromount-G (eBioscience) and immunofluorescent imaging was performed using a Leica (Wetzlar, Germany) DMRA fluorescence microscope equipped with a cooled camera. Images were acquired using Image Pro Plus (Media Cybernetics, Rockville, MD, USA) and composed in Adobe Photoshop CS5 (Adobe Systems, San Jose, CA, USA).

NF-κB binding enzyme-linked immunosorbent assay

After washing CLL cells in ice-cold PBS, nuclear lysates were prepared using the NucBuster protein extraction kit (Millipore, Billerica, MA, USA) according to the manufacturer's instructions. Protein concentration was measured with the BCA protein assay kit (Pierce, Thermo Fisher Scientific, Rockford, IL, USA) and 5 µg of protein was subsequently used as input for the TransAM NF-κB Family Transcription Factor Assay Kit, using provided antibodies for p65 and p52 according to the manufacturer's instructions. Signal intensity at 450 nm was then determined by spectrophotometer (Bio-Rad, Hercules, CA, USA).

MCL-1 knockdown

CLL cells were transfected using the AMAXA nucleofection technology (Amaxa, Cologne, Germany) with one of two different *MCL-1* siRNAs or control siRNA according to the manufacturer's instructions and as described.[46] In short, CLL cells were left to recover after thawing for at least 3 h at 37 °C in 5% CO_2. Cells (5.5×10^6) were resuspended in 100 µl human B-cell nucleofector kit solution (Lonza, Basel, Switzerland) and nucleofected with Silencer Select siRNAs (final concentration 3 µM) directed against *MCL-1* or a negative control (Ambion, Paisley, UK; catalog numbers s8585 (two CLL samples) and s8583 (three CLL samples) for MCL-1 and AM4635 as negative control) using program X-001. After transfection, cells were directly resuspended in pre-warmed $IMDM^{+/+}$ and plated in six-well plates to recover for at least 1h before commencing stimulation.

ABBREVIATIONS

4E-BP, eukaryotic translation initiation factor 4E-binding protein; AKT V-Akt murine thymoma viral oncogene homolog; APRIL, A proliferation-inducing ligand; BCL-2, B-cell lymphoma 2; BCL-X_L, B-cell lymphoma X large; BFL-1, pro-survival proteins BCL-2-related protein A1; CLL, chronic lymphocytic leukemia; eIF4, eukaryotic initiation factor 4; ERK, extracellular-signal-regulated kinase; GSK3, glycogen synthase kinase 3; LN, lymph node; MCL-1, induced myeloid leukemia cell differentiation protein; Mφ, macrophage; mTOR, mammalian target of rapamycin; NF-κB, nuclear factor of kappa light polypeptide gene enhancer in B cells; PI3K, phosphoinositide 3-kinase; PIM, proto-oncogene serine/threonine-protein kinase; S6, ribosomal protein S6.

CONFLICT OF INTEREST

The authors declare no conflict of interest.

ACKNOWLEDGEMENTS

We thank Richard Volckmann for his help with the analysis of the microarray data, Jannie Borst for providing the BFL-1 antibody and Steven Pals for providing us with the CLL LN slides. APK is a Dutch Cancer Foundation fellow. This work was supported by the Dutch Cancer Foundation (Dutch Cancer Society Clinical Fellowship UVA 2011-5097).

REFERENCES

1 Burger JA. Nurture versus nature: the microenvironment in chronic lymphocytic leukemia. *Hematol Am Soc Hematol Educ Program* 2011; **2011**: 96–103.
2 Hanna BS, McClanahan F, Yazdanparast H, Zaborsky N, Kalter V, Rossner PM *et al.* Depletion of CLL-associated patrolling monocytes and macrophages controls disease development and repairs immune dysfunction in vivo. *Leukemia* 2016; **30**: 570–579.
3 Pascutti MF, Jak M, Tromp JM, Derks IA, Remmerswaal EB, Thijssen R *et al.* IL-21 and CD40L signals from autologous T cells can induce antigen-independent proliferation of CLL cells. *Blood* 2013; **122**: 3010–3019.
4 Burger JA, Tsukada N, Burger M, Zvaifler NJ, Dell'Aquila M, Kipps TJ. Blood-derived nurse-like cells protect chronic lymphocytic leukemia B cells from spontaneous apoptosis through stromal cell-derived factor-1. *Blood* 2000; **96**: 2655–2663.
5 Nishio M, Endo T, Tsukada N, Ohata J, Kitada S, Reed JC *et al.* Nurse-like cells express BAFF and APRIL, which can promote survival of chronic lymphocytic leukemia cells via a paracrine pathway distinct from that of SDF-1alpha. *Blood* 2005; **106**: 1012–1020.
6 van Attekum MHA, Terpstra S, Reinen E, Kater AP, Eldering E. Macrophage-mediated chronic lymphocytic leukemia cell survival is independent of APRIL signaling. *Cell Death Discov* 2016; **2**: 16020.
7 Smit LA, Hallaert DY, Spijker R, de Goeij B, Jaspers A, Kater AP *et al.* Differential Noxa/Mcl-1 balance in peripheral versus lymph node chronic lymphocytic leukemia cells correlates with survival capacity. *Blood* 2007; **109**: 1660–1668.
8 Hallaert DY, Jaspers A, van Noesel CJ, van Oers MH, Kater AP, Eldering E. c-Abl kinase inhibitors overcome CD40-mediated drug resistance in CLL: implications for therapeutic targeting of chemoresistant niches. *Blood* 2008; **112**: 5141–5149.
9 Kitada S, Zapata JM, Andreeff M, Reed JC. Bryostatin and CD40-ligand enhance apoptosis resistance and induce expression of cell survival genes in B-cell chronic lymphocytic leukaemia. *Br J Haematol* 1999; **106**: 995–1004.
10 Tromp JM, Tonino SH, Elias JA, Jaspers A, Luijks DM, Kater AP *et al.* Dichotomy in NF-kappaB signaling and chemoresistance in immunoglobulin variable heavy-chain-mutated versus unmutated CLL cells upon CD40/TLR9 triggering. *Oncogene* 2010; **29**: 5071–5082.
11 Vogler M, Butterworth M, Majid A, Walewska RJ, Sun XM, Dyer MJ *et al.* Concurrent up-regulation of BCL-XL and BCL2A1 induces approximately 1000-fold resistance to ABT-737 in chronic lymphocytic leukemia. *Blood* 2009; **113**: 4403–4413.
12 Olsson A, Norberg M, Okvist A, Derkow K, Choudhury A, Tobin G *et al.* Upregulation of bfl-1 is a potential mechanism of chemoresistance in B-cell chronic lymphocytic leukaemia. *Br J Cancer* 2007; **97**: 769–777.
13 Awan FT, Kay NE, Davis ME, Wu W, Geyer SM, Leung N *et al.* Mcl-1 expression predicts progression-free survival in chronic lymphocytic leukemia patients treated with pentostatin, cyclophosphamide, and rituximab. *Blood* 2009; **113**: 535–537.
14 Kitada S, Andersen J, Akar S, Zapata JM, Takayama S, Krajewski S *et al.* Expression of apoptosis-regulating proteins in chronic lymphocytic leukemia: correlations with *in vitro* and *in vivo* chemoresponses. *Blood* 1998; **91**: 3379–3389.
15 Saxena A, Viswanathan S, Moshynska O, Tandon P, Sankaran K, Sheridan DP. Mcl-1 and Bcl-2/Bax ratio are associated with treatment response but not with Rai stage in B-cell chronic lymphocytic leukemia. *Am J Hematol* 2004; **75**: 22–33.
16 Pepper C, Lin TT, Pratt G, Hewamana S, Brennan P, Hiller L *et al.* Mcl-1 expression has in vitro and in vivo significance in chronic lymphocytic leukemia and is associated with other poor prognostic markers. *Blood* 2008; **112**: 3807–3817.
17 Cross DA, Alessi DR, Cohen P, Andjelkovich M, Hemmings BA. Inhibition of glycogen synthase kinase-3 by insulin mediated by protein kinase B. *Nature* 1995; **378**: 785–789.
18 Ma XM, Blenis J. Molecular mechanisms of mTOR-mediated translational control. *Nat Rev Mol Cell Biol* 2009; **10**: 307–318.
19 Ballou LM, Selinger ES, Choi JY, Drueckhammer DG, Lin RZ. Inhibition of mammalian target of rapamycin signaling by 2-(morpholin-1-yl)pyrimido[2,1-alpha] isoquinolin-4-one. *J Biol Chem* 2007; **282**: 24463–24470.

20 Thoreen CC, Kang SA, Chang JW, Liu Q, Zhang J, Gao Y *et al.* An ATP-competitive mammalian target of rapamycin inhibitor reveals rapamycin-resistant functions of mTORC1. *J Biol Chem* 2009; **284**: 8023–8032.
21 Castillo JJ, Furman M, Winer ES. CAL-101: a phosphatidylinositol-3-kinase p110-delta inhibitor for the treatment of lymphoid malignancies. *Expert Opin Investig Drugs* 2012; **21**: 15–22.
22 Maurer U, Charvet C, Wagman AS, Dejardin E, Green DR. Glycogen synthase kinase-3 regulates mitochondrial outer membrane permeabilization and apoptosis by destabilization of MCL-1. *Mol Cell* 2006; **21**: 749–760.
23 Mojsa B, Lassot I, Desagher S. Mcl-1 ubiquitination: unique regulation of an essential survival protein. *Cells* 2014; **3**: 418–437.
24 Baudot AD, Jeandel PY, Mouska X, Maurer U, Tartare-Deckert S, Raynaud SD *et al.* The tyrosine kinase Syk regulates the survival of chronic lymphocytic leukemia B cells through PKCdelta and proteasome-dependent regulation of Mcl-1 expression. *Oncogene* 2009; **28**: 3261–3273.
25 Masek T, Valasek L, Pospisek M. Polysome analysis and RNA purification from sucrose gradients. *Methods Mol Biol* 2011; **703**: 293–309.
26 Prevot D, Darlix JL, Ohlmann T. Conducting the initiation of protein synthesis: the role of eIF4G. *Biol Cell* 2003; **95**: 141–156.
27 Vary TC, Lynch CJ. Nutrient signaling components controlling protein synthesis in striated muscle. *J Nutr* 2007; **137**: 1835–1843.
28 Ueda T, Sasaki M, Elia AJ, Chio II, Hamada K, Fukunaga R *et al.* Combined deficiency for MAP kinase-interacting kinase 1 and 2 (Mnk1 and Mnk2) delays tumor development. *Proc Natl Acad Sci USA* 2010; **107**: 13984–13990.
29 Jefferies HB, Fumagalli S, Dennis PB, Reinhard C, Pearson RB, Thomas G. Rapamycin suppresses 5'TOP mRNA translation through inhibition of p70s6k. *EMBO J* 1997; **16**: 3693–3704.
30 Fox CJ, Hammerman PS, Cinalli RM, Master SR, Chodosh LA, Thompson CB. The serine/threonine kinase Pim-2 is a transcriptionally regulated apoptotic inhibitor. *Genes Dev* 2003; **17**: 1841–1854.
31 Wang X, McCullough KD, Franke TF, Holbrook NJ. Epidermal growth factor receptor-dependent Akt activation by oxidative stress enhances cell survival. *J Biol Chem* 2000; **275**: 14624–14631.
32 Takai S, Tokuda H, Hanai Y, Kozawa O. Activation of phosphatidylinositol 3-kinase/Akt limits FGF-2-induced VEGF release in osteoblasts. *Mol Cell Endocrinol* 2007; **267**: 46–54.
33 Su CC, Lin YP, Cheng YJ, Huang JY, Chuang WJ, Shan YS *et al.* Phosphatidylinositol 3-kinase/Akt activation by integrin-tumor matrix interaction suppresses Fas-mediated apoptosis in T cells. *J Immunol* 2007; **179**: 4589–4597.
34 Delgado-Martin C, Escribano C, Pablos JL, Riol-Blanco L, Rodriguez-Fernandez JL. Chemokine CXCL12 uses CXCR4 and a signaling core formed by bifunctional Akt, extracellular signal-regulated kinase (ERK)1/2, and mammalian target of rapamycin complex 1 (mTORC1) proteins to control chemotaxis and survival simultaneously in mature dendritic cells. *J Biol Chem* 2011; **286**: 37222–37236.
35 Johansson S, Svineng G, Wennerberg K, Armulik A, Lohikangas L. Fibronectin-integrin interactions. *Front Biosci* 1997; **2**: d126–d146.
36 Yamada KM, Even-Ram S. Integrin regulation of growth factor receptors. *Nat Cell Biol* 2002; **4**: E75–E76.
37 Balkwill F. Cancer and the chemokine network. *Nat Rev Cancer* 2004; **4**: 540–550.
38 Martelli AM, Evangelisti C, Chappell W, Abrams SL, Basecke J, Stivala F *et al.* Targeting the translational apparatus to improve leukemia therapy: roles of the PI3K/PTEN/Akt/mTOR pathway. *Leukemia* 2011; **25**: 1064–1079.
39 Mills JR, Hippo Y, Robert F, Chen SM, Malina A, Lin CJ *et al.* mTORC1 promotes survival through translational control of Mcl-1. *Proc Natl Acad Sci USA* 2008; **105**: 10853–10858.
40 Longo PG, Laurenti L, Gobessi S, Sica S, Leone G, Efremov DG. The Akt/Mcl-1 pathway plays a prominent role in mediating antiapoptotic signals downstream of the B-cell receptor in chronic lymphocytic leukemia B cells. *Blood* 2008; **111**: 846–855.
41 Martinez A, Sese M, Losa JH, Robichaud N, Sonenberg N, Aasen T *et al.* Phosphorylation of eIF4E confers resistance to cellular stress and DNA-damaging agents through an interaction with 4E-T: a rationale for novel therapeutic approaches. *PLoS One* 2015; **10**: e0123352.
42 Pradelli LA, Beneteau M, Chauvin C, Jacquin MA, Marchetti S, Munoz-Pinedo C *et al.* Glycolysis inhibition sensitizes tumor cells to death receptors-induced apoptosis by AMP kinase activation leading to Mcl-1 block in translation. *Oncogene* 2010; **29**: 1641–1652.
43 Balakrishnan K, Burger JA, Quiroga MP, Henneberg M, Ayres ML, Wierda WG *et al.* Influence of bone marrow stromal microenvironment on forodesine-induced responses in CLL primary cells. *Blood* 2010; **116**: 1083–1091.
44 Allen JC, Talab F, Zuzel M, Lin K, Slupsky JR. c-Abl regulates Mcl-1 gene expression in chronic lymphocytic leukemia cells. *Blood* 2011; **117**: 2414–2422.
45 Buggins AG, Pepper C, Patten PE, Hewamana S, Gohil S, Moorhead J *et al.* Interaction with vascular endothelium enhances survival in primary chronic lymphocytic leukemia cells via NF-kappaB activation and *de novo* gene transcription. *Cancer Res* 2010; **70**: 7523–7533.
46 Vogler M, Dinsdale D, Sun XM, Young KW, Butterworth M, Nicotera P *et al.* A novel paradigm for rapid ABT-737-induced apoptosis involving outer mitochondrial membrane rupture in primary leukemia and lymphoma cells. *Cell Death Differ* 2008; **15**: 820–830.

Supplementary Information accompanies this paper on the Oncogene website (http://www.nature.com/onc)